ACS OMEGA

http://pubs.acs.org/journal/acsodf

Article

Effective Synthesis of *m*-Xylylene Dicarbamate via Carbonylation of *m*-Xylylene Diamine with Ethyl Carbamate over Hierarchical TS-1 Catalysts

Junya Cao,[§] Junya Zhou,[§] Liguo Wang,* and Yan Cao

Cite This: *ACS Omega* 2022, 7, 23851−23857

Read Online

ACCESS | Metrics & More | Article Recommendations

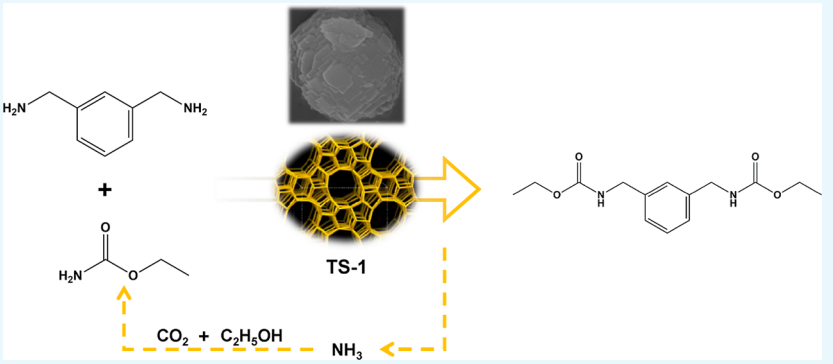

ABSTRACT: Carbonylation of *m*-xylylene diamine (XDA) with ethyl carbamate to produce *m*-xylylene dicarbamate (XDC), which is the crucial intermediate for the production of *m*-xylylene diisocyanate (XDI), over the hierarchical TS-1 (HTS-1) zeolite catalyst was studied. The catalysts were characterized by Brunauer−Emmett−Teller, X-ray diffraction, Fourier transform infrared spectroscopy, scanning electron microscopy, and temperature-programed desorption of ammonia techniques systematically. The results showed that the high performance of HTS-1 could be attributed to the weak acidity and high V_{meso}/V_{total} ratio of the catalyst. Impacts of reaction time and reusage on the HTS-1 catalyst were also investigated. Under 6 h and 200 °C, XDA conversion could reach 100% with 88.5% XDC yield. Furthermore, partial loss of Ti active sites with Lewis acidity on the catalyst surface led to the decrease of XDC yield during recycling. Moreover, a possible reaction mechanism for the title reaction was primarily proposed.

1. INTRODUCTION

m-Xylylene diisocyanate (XDI) is a kind of aliphatic isocyanate with the structure of the $-CH_2-$ group between the benzene ring and isocyanate group. This structure makes it resistant to yellowing, thus being applied in the field of high-grade coatings, medical polyurethane, and so forth. Furtherly, because of the similar refractive index between human eyes and resin flakes made from XDI-based polyurethanes, it is widely used in the field of high-grade polyurethane glasses.[1,2]

Industrially, isocyanate is produced via the carbonylation of phosgene with *m*-xylylene diamine (XDA),[3,4] which has the disadvantages of extreme toxicity and the formation of corrosive HCl. Among various phosgene-free methods, thermal decomposition of carbamate is considered as the most effective way, which generally contains two consecutive processes: (1) first, the synthesis of the intermediate of carbamate as the precursor for thermal decomposition and (2) subsequently, the thermal decomposition of carbamate to isocyanate with the depletion of alcohol during the reaction.[5,6] Therefore, the synthesis of carbamate is very important for the production of isocyanate via a phosgene-free route.

Traditionally, carbamates were synthesized by alcoholysis of substituted ureas, oxidative carbonylation of amines, and reductive carbonylation of nitro-compounds. However, these routes suffered from high temperature, high cost of the noble catalyst, or high risk in safety.[7] In order to overcome the aforementioned problems, the carbonylation of diamines with low-molecular-weight carbamates has become an attractive route in recent years. On account of these reasons, an efficient synthesis route for *m*-xylylene dicarbamate (XDC) from the reaction of XDA with ethyl carbamate (EC) was developed, as shown in Scheme 1. Because EC could be readily synthesized

Received: April 23, 2022
Accepted: June 15, 2022
Published: June 28, 2022

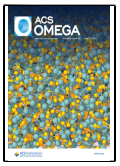

https://doi.org/10.1021/acsomega.2c02535
ACS Omega 2022, 7, 23851−23857

Scheme 1. Synthesis Route of XDC from the Reaction of XDA with EC

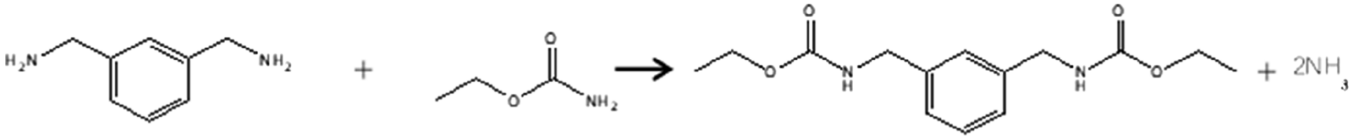

via alcoholysis of urea, this route also can be considered as CO_2 indirect utilization, in the process of which CO_2 was deemed as the original carbonylation reagent in the whole chains.[8−10] It should be noted in the previous results that the efficiency of the reaction is limited without an effective catalyst. This issue is expected to be overcome by the involvement of a proper catalyst.

Over the past few years, carbamate syntheses over several homogeneous and heterogeneous catalysts have been reported, such as $Mg_2Zr_xAl_{1-x}$−MMO,[11] Ga_2O_3,[12] Mg−Al−Y,[13] Cu-CPO-27,[14] alkali-treated zeolites,[15] Ce−Zn,[16] tungstophosphoric acid (TPA/K30),[17] $Mn(OAc)_2$,[18] Pd/ZrO_2,[19] $NaOCH_3$,[20] $CuCl_2$/ionic liquids,[21] $[BSO_3HMIm][OTf]$,[22] Se,[23] AlSBA-15,[24] Zn/SiO_2,[25] and 3-amino-1,2,4-triazole potassium (KATriz).[26] However, difficulties in homogeneous catalyst separation and low catalytic activity for the heterogeneous catalysts resulted in difficulties in the scale-up process. Therefore, an effective heterogeneous catalyst is still highly desired.[7]

Titanium silicate (TS-1) zeolite possesses the properties of high total surface area, thermal stability, low toxicity, reusability, ion exchange capability, and easy handling. Therefore, it is widely applied in the reaction of oxidation, epoxidation, alkylation, acylation, and cyclic condensation.[27−35] However, the particle size of traditional TS-1 nanoparticles is usually small, thus resulting in limitations of intracrystalline diffusion.

Hierarchically porous zeolites, especially hierarchical TS-1 (HTS-1) zeolites with a MFI topological structure, have received great attention in catalytic oxidation processes because of their microporous and mesoporous/macroporous characteristics which enhance the mass transport and improve catalytic performance. Srivastava et al. used titanium silicate to catalyze the formation of carbamates using CO_2 as the raw materials, and it showed good results.[36] Therefore, the application of the HTS-1 catalyst in XDC production is of great significance.

Herein, we report an efficient and environment-friendly route for the synthesis of XDC. In this work, HTS-1 catalysts with different Ti contents were prepared by the hydrothermal method and then used in the carbonylation of XDA to XDC for the first time. The physicochemical properties of the catalysts were characterized by the Brunauer−Emmett−Teller (BET) method, X-ray diffraction (XRD), Fourier transform infrared (FT-IR) spectroscopy, scanning electron microscopy (SEM), and temperature-programed desorption of ammonia (NH_3-TPD). The effects of reaction time on the catalytic performance, as well as the reuse of the HTS-1 catalyst, were studied. Furthermore, the reaction mechanism was studied.

2. EXPERIMENTAL SECTION

2.1. Synthesis of Hierarchically Porous HTS-1 Catalysts [TS-1-(0), TS-1-(1), TS-1-(2), and TS-1-(3)]. Tetrabutyltitanate was mixed with tetraethylorthosilicate with the molar ratio of the composition being $100SiO_2/nTiO_2$ (n = 0, 1.19, 2.38, and 3.57) at 0 °C for 3 h under stirring, followed by addition of tetrapropylammonium hydroxide (TPAOH) (25% wt) with the molar ratio of the composition being $100SiO_2/30TPAOH/124H_2O$ at 0 °C for 12 h under stirring. The as-obtained mixture was crystalized at 180 °C for 2 days. The sample was washed with distilled water and dried overnight at 80 °C, followed by calcination at 550 °C for 6 h. Then, the resulting products were named TS-1-(0), TS-1-(1), TS-1-(2), and TS-1-(3), respectively.

2.2. Characterizations. Powder XRD patterns were recorded using a Bruker D8 ADVANCE X-ray diffractometer with CuKa radiation (k = 0.15406 nm) over a 2θ range of 5−90°. The working voltage and applied currents were 40 kV and 40 mA, respectively. SEM images of the samples were obtained using Bruker Nova NanoSEM operated at 5.0 kV. Nitrogen adsorption−desorption isotherms were measured at 77 K using a Micromeritics ASAP 2020 M instrument, and the sample was outgassed at 300 °C for 10 h prior to measurement.

N_2-physisorption was carried out at 77 K by using an adsorption apparatus (ASAP 2460). Before the analysis, the samples were evacuated at 200 °C for 4 h in vacuum. The specific surface area (SBET) was determined by the BET equation. The total pore volume (V_{pore}) was obtained based on the stored nitrogen volume when the relative pressure was 0.99. The S_{micro}, S_{meso}, V_{micro}, and V_{meso} were calculated by the t-plot method. The element contents were analyzed with inductively coupled plasma emission spectroscopy (ICP, Varian 710-ES) after the sample was solved. The FT-IR spectra of the catalysts were collected using a Nicolet NEXUS 670 FT-IR spectrometer, and the sample to be measured was ground with KBr and pressed into thin wafers.

The yield of the product in the sample was calculated through the data obtained by gas chromatography. The conversion of XDA and selectivity of XDC were calculated as follows

$$\text{Conv. (XDA) (\%)} = \frac{n_0(\text{XDA}) - n(\text{XDA})}{n_0(\text{XDA})} \times 100\% \quad (1)$$

$$\text{Sel. (XDC) (\%)} = \frac{n(\text{XDC})}{n_0(\text{XDA}) - n(\text{XDA})} \times 100\% \quad (2)$$

where n_0(XDA) is the molar amount of XDA added before the reaction, n(XDA)is the molar amount of XDA remaining after the reaction, and n(XDC) is the molar amount of the target product produced by the reaction.

In this paper, in order to facilitate the evaluation of catalyst conversion efficiency, the value is defined as the amount of XDC (mmol) converted per hour per titanium content (mole), and the unit of this value is $mmol_{XDC}{\cdot}mol_{Ti}{\cdot}h^{-1}$, and the calculation formula is as follows

$$\text{catalyst activity} = \frac{n(\text{XDC})}{n_{\text{Ti}} \times t_r} \times 1000 \quad (3)$$

https://doi.org/10.1021/acsomega.2c02535
ACS Omega 2022, 7, 23851−23857

Table 1. Influence of Different Loadings on Textural Properties and Catalytic Performance[a]

catalyst	Ti (wt %)	S_{BET} (m^2/g)	S_{micro} (m^2/g)	S_{meso} (m^2/g)	S_{meso}/S_{total}	V_{total} (cm^3/g)	V_{micro} (cm^3/g)	V_{meso} (cm^3/g)	V_{meso}/V_{total}
TS-1-(0)	0	398.3	276.5	121.8	0.306	0.213	0.134	0.076	0.357
TS-1-(1)	0.85	463.1	357.5	105.6	0.228	0.230	0.162	0.068	0.296
TS-1-(2)	1.63	466.8	345.1	121.7	0.261	0.265	0.168	0.096	0.362
TS-1-(3)	1.90	419.0	253.1	165.9	0.396	0.209	0.122	0.087	0.416

[a]The contents of Ti were detected by ICP spectroscopy.

where n(XDC) is the amount of XDC produced by the reaction (mol), n_{Ti} is the titanium content of the catalyst added to the reaction system (mol), and t_r is the reaction time (h).

2.3. Catalytic Reaction and Recyclability. All reactions were conducted in a 100 mL stainless-steel autoclave equipped with a magnetic stirrer. Approximately 1.36 g (0.01 mol) of XDA, 4.45 g (0.07 mol) of EC, and 0.2 g of [14.7 wt % (based on XDA)] the catalyst were charged successively into a round-bottomed flask and reacted at 463−483 K with stirring for 1−8 h. After the reaction, the flask was cooled down to room temperature. About 50 mL of methanol was added to dissolve XDA, XDC, and other byproducts. The insoluble byproducts were removed by filtration or centrifugation if needed.

3. RESULTS AND DISCUSSION

The surface areas and pore volumes of HTS-1 samples with different loadings are presented in Table 1. The as-prepared HTS-1 catalysts were found to have a relatively large surface area (398−419 m^2/g) and total volume (0.213−0.265 cm^3/g), which was expected to expose abundant active sites. Noteworthy to say, abundant mesopores in the HTS-1 were formed during catalyst preparation. According to the calculation result, the ratios of the mesopore volume to total volume (V_{meso}/V_{total}) of these samples are all higher than 20%, suggesting the hierarchical structure of these TS-1 catalysts.

Catalyst acidities of various TS catalysts were measured by NH_3-TPD. In the previous report, the ethoxy carbonylation of diamine was proven to be an acid catalytic reaction, and an acidic catalyst can promote this reaction efficiently.[6] It is generally accepted that two kinds of acid sites exited on the surface of TS-1 zeolites, namely, the weak acid site and the

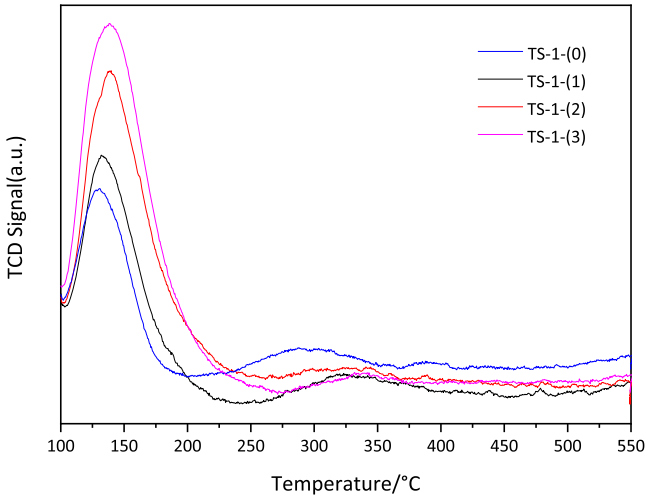

Figure 1. NH_3-TPD patterns of HTS-1 catalysts.

Table 2. Influence of Reaction Time on Catalytic Performance[a]

catalyst	reaction time (h)	XDA Conv. (%)	XDC yield (%)	XDC Sel. (%)	catalyst activity ($mmol_{XDC}/mol_{Ti}$·h)
blank	1	100	26.4	26.4	
TS-1-(0)	1	100	56.6	56.6	
TS-1-(1)	1	100	51.3	51.3	144.1×10^3
TS-1-(2)	1	100	59.8	59.8	87.7×10^3
TS-1-(3)	1	100	61.3	61.3	77.3×10^3
TS-1-(3)	2	100	65.8	65.8	41.5×10^3
TS-1-(3)	4	100	79.6	79.6	25.1×10^3
TS-1-(3)	6	100	88.5	88.5	18.6×10^3

[a]Reaction conditions: 200 °C, 450 rpm, pressure 1.8 MPa. Catalyst activity: the amounts of XDC formed per mole of Ti per hour.

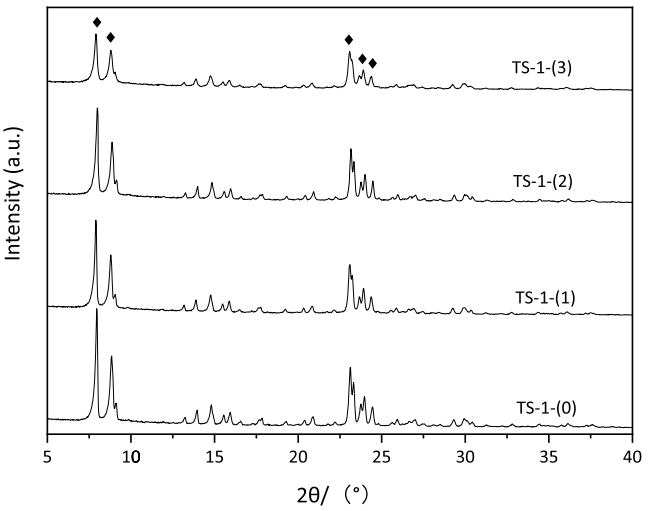

Figure 2. XRD patterns of HTS-1 catalysts.

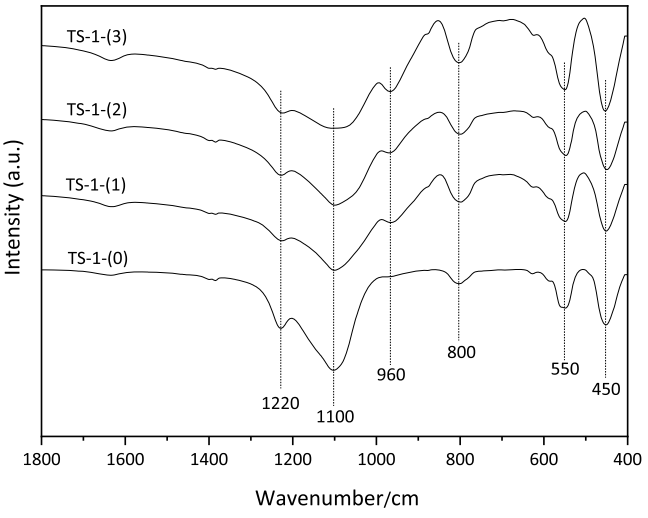

Figure 3. FT-IR patterns of HTS-1 catalysts.

https://doi.org/10.1021/acsomega.2c02535
ACS Omega 2022, 7, 23851−23857

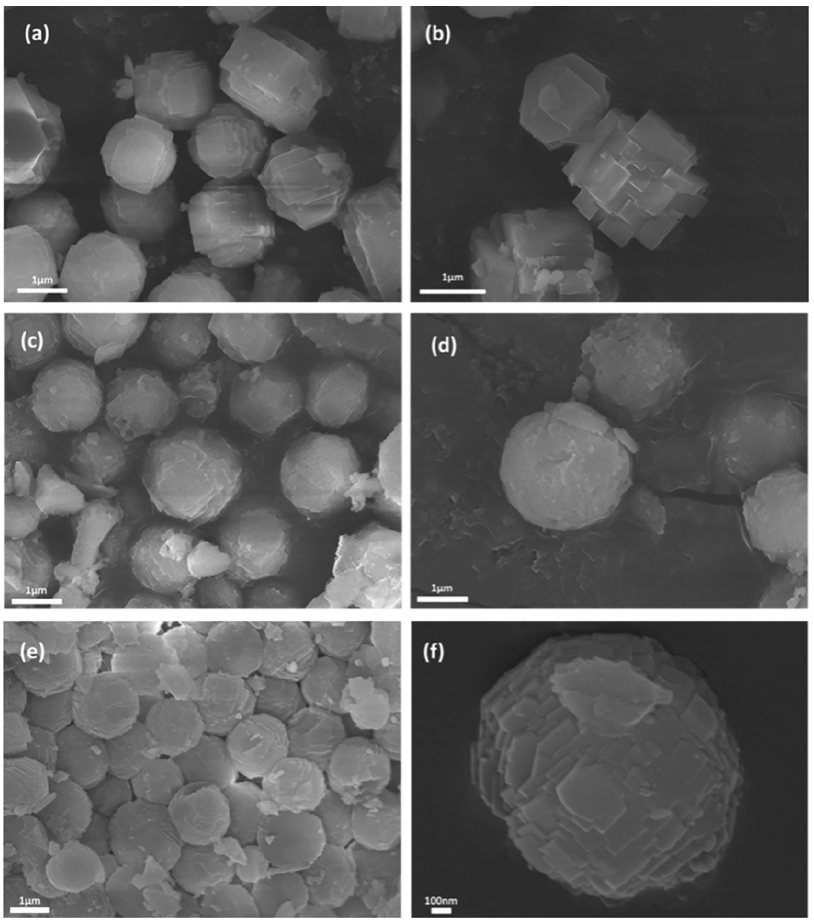

Figure 4. SEM images of TS-1-(1) (a,b); TS-1-(2) (c,d); TS-1-(3) (e,f).

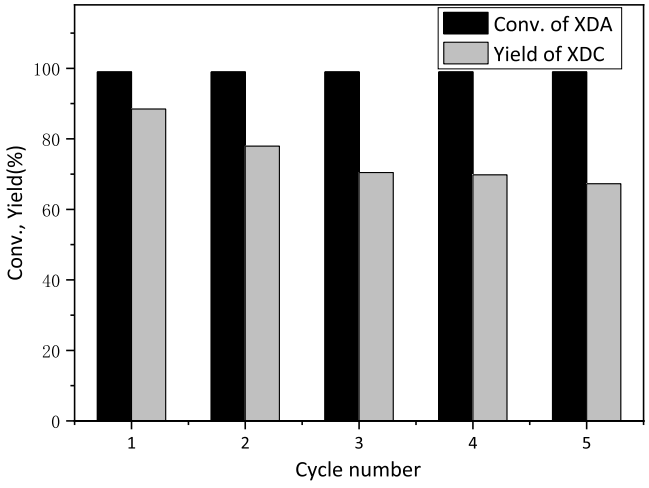

Figure 5. Recycling graph for TS-1-(3) for the synthesis of XDC.

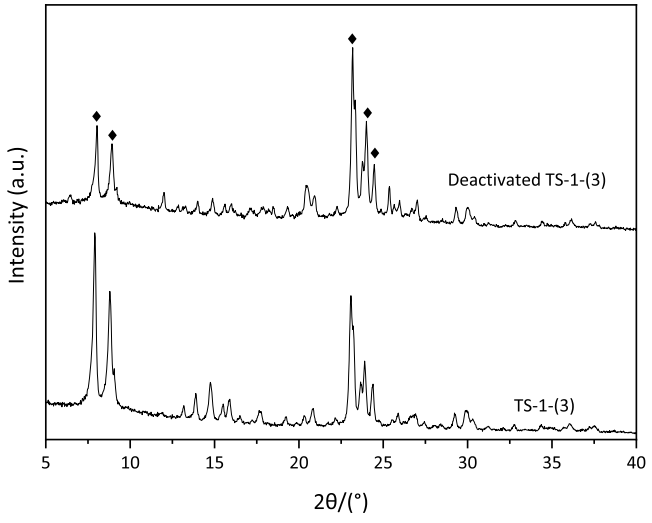

Figure 6. XRD patterns of TS-1-(3) and deactivated TS-1-(3).

strong acid site, which originated from the framework Ti(IV) ions and the silanol groups at crystal defects, respectively.[37]

NH_3-TPD profiles for HTS-1 catalysts in Figure 1 showed two major desorption zones approximately at 130−140 °C for weak acidic sites and 285−345 °C for strong acid sites. All the HTS-1 catalysts clearly exhibited major weak acidic sites and a small proportion of strong acidic sites. The weak acidity increased for various HTS-1 catalysts in the sequence TS-1-(1) < TS-1-(2) < TS-1-(3), which was well consistent with the trends of XDC yields (Table 2), suggesting that the role of weak acidity of HTS-1 is significant in the catalytic performance. Meanwhile, the bare MFI without Ti loading [TS-1-(0)] exhibited slightly weak acidity. Figure 2 displays the XRD patterns of HTS-1 catalysts. All of these samples exhibited typical diffraction peaks at 2θ = 7.8, 8.8, 23.2, 23.8, and 24.3°, which are coincident with the MFI zeolitic topology.

Then, FT-IR analysis was carried out for the HTS-1 samples, and the result in Figure 3 shows that the framework of the

https://doi.org/10.1021/acsomega.2c02535
ACS Omega 2022, 7, 23851−23857

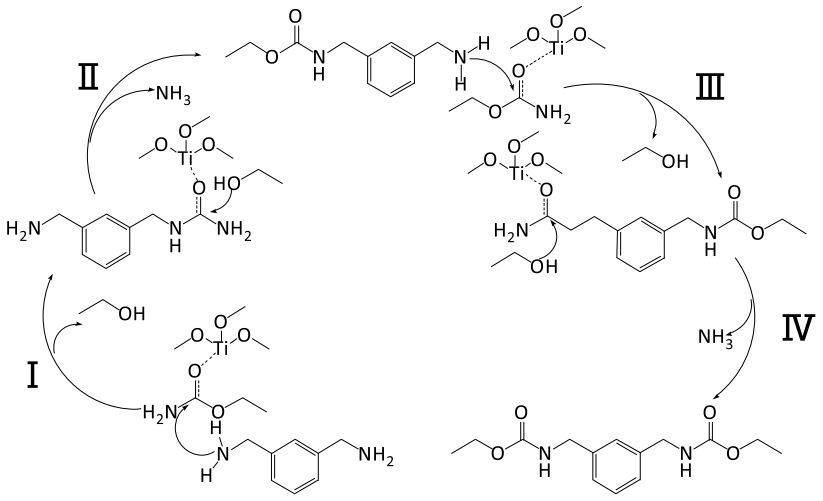

Figure 7. Proposed reaction mechanism for the reaction of XDA, EC, and ethanol over the HTS-1 catalyst.

zeolite was retained by the evidence of characteristic peaks of internal vibrations of (Si, Ti) O_4 (1100 and 800 cm^{-1}), double-ring tetrahedral vibrations (1230 cm^{-1}), and asymmetric stretching of SiO_4 and TiO_4 tetrahedra (550 cm^{-1}). What is more, compared with TS-1(0), because of the incorporation of Ti ions, TS-1(1), TS-1(2), and TS-1(3) all showed the absorption peak of Si−O−Ti at 960 cm^{-1} and increased in intensity with increasing Ti content. This is because of the overlap of the Si−(OH) stretching mode of the silanol groups of silica with the Si−O−Ti asymmetric stretching mode involving Ti dissolved into the silica framework.[38] Figure 4 shows the SEM images of HTS-1 samples synthesized with different Ti loading levels. The results showed that different from the reported smooth surface of traditionally prepared microporous TS-1, all the HTS-1 samples with a mean size of around 1.5 μm showed uniform particles with a rough surface and layered structure, which is the characteristic morphology of the HTS-1 catalyst.

The effects of the various hierarchical TS catalysts with varying Ti loadings on the ethoxy carbonylation of XDA with EC were further tested. First, when a blank reaction was carried out without any catalyst, only a 26.4% XDC yield was obtained. After adding pure MFI without Ti species, the XDC yield sharply increased to 56.6%, whereas the bare MFI without Ti loading [TS-1-(0)] possessed slightly weak acidity but exhibited a relatively higher XDC yield in comparison with the blank result without any catalyst, which might be attributed to the influence of its higher strong acidity derived from Si−OH groups. However, the XDC yield also decreased to 51.3% for TS-1-(1) after introduction of a small amount of Ti, that is, 0.85%. It should be noted that pure MFI exhibits a V_{meso}/V_{total} of 0.357[TS-1-(0)], while the TS-1-(1) catalyst showed an obviously lower V_{meso}/V_{total} ratio of 0.296 after introduction of 0.85 wt % Ti. With a further increase of Ti from 0.85% in TS-1-(1) to 1.90% in TS-1-(3), the V_{meso}/V_{total} increased from 0.296 to 0.416, and a higher XDC yield of 61.3% was obtained over TS-1-(3). This indicated that XDC yield has a positive correlation with the V_{meso}/V_{total} ratio, indicating that a higher proportion of mesopore volume facilitated the reaction.[39] On account of these reasons, the optimum catalyst is TS-1-(3) with a Ti content of 1.90%

The catalyst TS-1-(3) was used to catalyze the reaction of XDA with EC at a temperature of 200 °C. The results in Table 2 show that the yield of XDC increased from 61.3 to 88.5% upon increasing the time from 1 to 6 h. The reusability of heterogeneous catalysts is an important parameter for practical applications. Therefore, the recyclability of the TS-1-(3) catalyst was tested and the results are shown in Figure 5. The reaction for the synthesis of XDC was carried out under conditions of 200 °C reaction temperature, 6 h reaction time, 14.7 wt % catalyst, and a molar ratio of XDA/EC = 1:7. The catalyst was recycled five times by centrifugation and then directly used in the next run. It can be seen that XDA conversion remained at 100%. In contrast, the XDC yield decreased obviously in the second and third runs and then decreased slightly in the fourth and fifth runs. The ICP spectroscopy results showed that after recycling for five runs, the Ti content decreased from 1.90 to 1.71%. Moreover, compared with the fresh catalyst, the used catalyst did not show any change in the XRD pattern (Figure 6). These results indicate that the structure of the catalyst is maintained after being used five times, and the decrease in the performance of the HTS-1 catalyst was probably on account of the loss of Ti active sites with Lewis acidity on the catalyst surface during recyclability. This finding could provide helpful information for further improvement of the catalysts to meet the requirement of the practical application.

For the carbonylation reaction of a diamine with carbamates, two possible mechanisms have been proposed in the previous literature, that is, the transesterification pathway and alcoholysis pathway. Deng et al. used quasi-in situ FT-IR spectroscopy to investigate the reaction pathway and verified the formation of substituted urea as the key intermediate,[6] while the previous work of our group also gave the experimental evidence for further identification of the alcoholysis reaction mechanism of the carbonylation reaction.[7] What is more, no xylene monocarbamate intermediate was detected after the ethoxy carbonylation of XDA with EC by GC in this reaction. Therefore, the reaction mechanism is also considered as an alcoholysis pathway, as shown in Figure 7. The first is the formation of the urea intermediate with the removal of an alcohol molecule, followed by the formation of N-substituted carbamate in the second step with the contemporary elimination of an ammonia molecule. Generally, the amino group of XDA attacks the carbon in the carbonyl group of EC and (3-ureidomethyl-benzyl)-urea (XDU) is generated by

https://doi.org/10.1021/acsomega.2c02535
ACS Omega 2022, 7, 23851−23857

delivering the ethoxy group. Finally, ethanol attacks the amino group of XDU to form XDC.

4. CONCLUSIONS

In this work, HTS-1 catalysts with different Ti contents were produced via the hydrothermal method and used in the carbonylation of XDA to XDC for the first time. The physicochemical properties of the catalyst were characterized by different techniques, and it turned out that the catalyst exhibited a large external surface area with abundant mesoporous structures. The effects of reaction time on catalytic performance and reusability of the HTS-1 catalyst were studied. Among the catalysts tested, TS-1-(3) with a higher Ti content demonstrated better catalytic activity, and 100% XDA conversion with 88.5% XDC yield was achieved. Furthermore, the reaction mechanism was proposed as an alcoholysis pathway in which the urea intermediate was formed first, followed by the formation of N-substituted carbamate.

AUTHOR INFORMATION

Corresponding Author

Liguo Wang − *Key Laboratory of Green Process and Engineering, National Engineering Research Center of Green Recycling for Strategic Metal Resources. Institute of Process Engineering, Chinese Academy of Sciences, Beijing 100190, China;* orcid.org/0000-0002-8509-7950; Email: lgwang@ipe.ac.cn

Authors

Junya Cao − *China University of Mining & Technology, Beijing 100083, China*

Junya Zhou − *China University of Mining & Technology, Beijing 100083, China; Key Laboratory of Green Process and Engineering, National Engineering Research Center of Green Recycling for Strategic Metal Resources. Institute of Process Engineering, Chinese Academy of Sciences, Beijing 100190, China*

Yan Cao − *Key Laboratory of Green Process and Engineering, National Engineering Research Center of Green Recycling for Strategic Metal Resources. Institute of Process Engineering, Chinese Academy of Sciences, Beijing 100190, China*

Complete contact information is available at: https://pubs.acs.org/10.1021/acsomega.2c02535

Author Contributions

§J.C. and J.Z. contributed equally to this work and should be considered as co-first authors.

Notes

The authors declare no competing financial interest.

ACKNOWLEDGMENTS

We are grateful for the financial support from the "Transformational Technologies for Clean Energy and Demonstration", Strategic Priority Research Program of the Chinese Academy of Sciences, grant no. XDA 21030600, and Science and Technology Service Network Initiative, Chinese Academy of Sciences (KFJ-STS-QYZD-138).

REFERENCES

(1) Zang, M. G.; Du, W. P.; Wang, S. Study on Curing Technique for XDI/BES Polyurethane Lens. *Glass Enamel & Ophthalmic Opt.* **2021**, *49*, 6−12.

(2) Zhang, Y. W.; Wang, X. S.; Chen, Y. S. Preparation of Polythiourethane Optical Resin Based on 2,3-bis[(2-mercaptoethyl) thio]-1- propanethiol and 1,3-bis(isocyanan tomethyl) cyclohexane. *Glass Enamel & Ophthalmic Opt.* **2021**, *49*, 1−5.

(3) Dong, J.; Zhang, Y.; Li, S. Study on m-xylylene diisocyanate synthesis with triphosgene. *Chem. Res. Appl.* **2015**, *27*, 891−894.

(4) Wang, P.; Liu, S.; Deng, Y. Important Green Chemistry and Catalysis: Non-phosgene Syntheses of Isocyanates-Thermal Cracking Way. *Chin. J. Chem.* **2017**, *35*, 821−835.

(5) Ammer, M.; Cao, Y.; Li, H. Q. Zn-Co bimetallic supported ZSM-5 catalyst for phosgene-free synthesis of hexamethylene−1,6−diisocyanate by thermal decomposition of hexamethylene−1,6−dicarbamate. *Chin. J. Chem. Eng.* **2017**, *17*, 1760−1770.

(6) Shang, J.; Guo, X.; Shi, F.; Ma, Y.; Zhou, F.; Deng, Y. N-substituted carbamates syntheses with alkyl carbamates as carbonyl source over Ni-promoted Fe_3O_4 catalyst. *Chin. J. Catal.* **2011**, *279*, 328−336.

(7) Ammar, M.; Cao, Y.; Wang, L. Synthesis of hexamethylene-1,6-dicarbamate by methoxycarbonylation of 1,6-hexamethylene diamine with dimethyl carbonate over bulk and hybrid heteropoly acid catalyst. *Res. Chem. Intermed.* **2017**, *43*, 6951.

(8) Xin, S.; Wang, L.; Li, H.; Huang, K.; Li, F. Synthesis of diethyl carbonate from urea and ethanol over lanthanum oxide as a heterogeneous basic catalyst. *Fuel Process. Technol.* **2014**, *126*, 453−459.

(9) Sun, D. L.; Hong, Z. P.; Ye, J. H. Thermodynamic Analysis of Synthesis of Carbamates from Carbon Dioxide, Ammonia and Alcohols. *Spec. Petrochem.* **2016**, *57*, 153−158.

(10) Wang, L.; Li, H.; Xin, S.; Li, F. Generation of solid base catalyst from waste slag for the efficient synthesis of diethyl carbonate from ethyl carbamate and ethanol. *Catal. Commun.* **2014**, *50*, 49−53.

(11) Yan, T.; Bing, W.; Xu, M.; Li, Y.; Yang, Y.; Cui, G.; Yang, L.; Wei, M. Acid−base sites synergistic catalysis over Mg−Zr−Al mixed metal oxide toward synthesis of diethyl carbonate. *RSC Adv.* **2018**, *8*, 4695−4702.

(12) Shah, J.; Ratnasamy, P.; Carreon, M. Influence of the Nanostructure of Gallium Oxide Catalysts on Conversion in the Green Synthesis of Carbamates. *Catalysts* **2017**, *7*, 372.

(13) Wang, D.; Zhang, X.; Zhou, D.; Liu, S.; Wei, W. Influence of Y on the performance of Mg-Al-Y catalysts via hydrotalcite-like precursors for the synthesis of diethyl carbonate from ethyl carbamate and ethanol. *Fuel Process. Technol.* **2017**, *167*, 404−415.

(14) Nguyen, C. K.; Nguyen, N. B.; Chu, O. N.; Dang, H. V.; Nguyen, T. T.; Phan, N. T. S. A direct strategy to synthesize hybrid benzothiazole−carbamate moieties via O-acylation of phenols under metal−organic framework catalysis. *React. Chem. Eng.* **2017**, *2*, 669−678.

(15) Sun, Q.; Niu, R.; Wang, H.; Lu, B.; Zhao, J.; Cai, Q. Environmentally benign alcoholysis of urea and disubstituted urea to alkyl carbamates over alkali-treated zeolites. *Microporous Mesoporous Mater.* **2017**, *248*, 108−114.

(16) Shukla, K.; Srivastava, V. C. Diethyl carbonate synthesis by ethanolysis of urea using Ce-Zn oxide catalysts. *Fuel Process. Technol.* **2017**, *161*, 116−124.

(17) Tran, A. V.; Baik, J. H.; Baek, J. Montmorillonite K30 Supported Tungstophosphoric Acid as an Efficient Catalyst for Condensation Reaction of Methyl N-phenylcarbamate for Generating Diurethane. *Catal Lett* **2021**, DOI: 10.1007/s10562-021-03793-4.

(18) Zhao, L.; He, P.; Wang, L.; Ammar, M.; Cao, Y.; Li, H. Catalysts screening, optimization and mechanism studies of dimethylhexane-1,6-dicarbamate synthesis from 1,6-hexanediamine and dimethyl carbonate over $Mn(OAc)_2$ catalyst. *Catal. Today* **2017**, *281*, 392.

(19) Hussong, C.; Langanke, J.; Leitner, W. A green route to polyurethanes: oxidative carbonylation of industrially relevant aromatic diamines by CO_2-based methyl formate. *Green Chem.* **2020**, *22*, 8260−8270.

(20) Sun, D.-L.; Xie, S.-J.; Deng, J.-R.; Huang, C.-J.; Ruckenstein, E.; Chao, Z.-S. CH_3COONa as an effective catalyst for methoxycarbo-

nylation of 1,6-hexanediamine by dimethyl carbonate to dimethylhexane-1,6-dicarbamate. *Green Chem.* **2010**, *12*, 483−490.
(21) Li, M. C.; Du, C. Three-component Reactions of Propargyl Alcohols, Secondary Amines and CO_2 Catalyzed by $CuCl_2$/Ionic Liquids. *Mol. Catal.* **2019**, *33*, 542−550.
(22) Liu, S. M.; Wang, P. X.; Deng, Y. Q. Green non-phosgene process for manufacturing isocyanates. *Sci. Sin.: Chim.* **2020**, *50*, 235−244.
(23) Sun, D.-L.; Deng, J.-R.; Chao, Z.-S. Catalysis over zinc-incorporated berlinite ($ZnAlPO_4$) of the methoxycarbonylation of 1,6-hexanediamine with dimethyl carbonate to form dimethylhexane-1,6-dicarbamate. *Chem. Cent. J.* **2007**, *1*, 27.
(24) Li, H.-Q.; Cao, Y.; Li, X.-T.; Wang, L.-G.; Li, F.-J.; Zhu, G.-Y. Heterogeneous Catalytic Methoxycarbonylation of 1,6-Hexanediamine by Dimethyl Carbonate to Dimethylhexane-1,6-dicarbamate. *Ind. Eng. Chem. Res.* **2013**, *53*, 626−634.
(25) Zhang, L.; Li, H.; Li, F.; Pu, Y.; Zhao, N.; Xiao, F. Methoxycarbonylation of 1,6-hexanediamine with dimethyl carbonate to dimethylhexane-1,6-dicarbamate over Zn/SiO_2 catalyst. *RSC Adv.* **2016**, *6*, 51446−51455.
(26) Wang, P.; Fei, Y.; Li, Q.; Deng, Y. Effective synthesis of dimethylhexane-1,6-dicarbamate from 1,6-hexanediamine and dimethyl carbonate using 3-amino-1,2,4-triazole potassium as a solid base catalyst at ambient temperature. *Green Chem.* **2016**, *18*, 6681−6686.
(27) Le Bars, J.; Dakka, J.; Sheldon, R. A. Ammoximation of cyclohexanone and hydroxyaromatic ketones over titanium molecular sieves. *Appl. Catal., A* **1996**, *136*, 69−80.
(28) Ma, S. J.; Wen, L. S.; Li, L. S. Study on the Synthesis of the Titanosilicate Zeolite Molecular Sieve TS-2. *J. Jilin Univ. Sci. Ed.* **1996**, *1*, 81−84.
(29) Kerton, O. J.; Mcmorn, P.; Bethell, D.; King, F.; Hancock, F.; Burrows, A.; Kiely, C. J.; Ellwood, S.; Hutchings, G. Effect of structure of the redox molecular sieve TS-1 on the oxidation of phenol, crotyl alcohol and norbornylene. *Phys. Chem. Chem. Phys.* **2005**, *7*, 2671−2678.
(30) Puziy, A. M.; Bengtsson, G. B.; Hansen, H. S. Characterization of novel adsorbents for radiostrontium reduction in foods. *J. Radioanal. Nucl. Chem.* **1999**, *240*, 101−107.
(31) Wróblewska, A. The epoxidation of limonene over the TS-1 and Ti-SBA-15 catalysts. *Molecules* **2014**, *19*, 19907−19922.
(32) Zhang, Y.; Wang, Y.; Bu, Y.; Wang, L.; Mi, Z.; Wu, W.; Min, E.; Fu, S.; Zhu, a. Z. Reaction mechanism of the ammoximation of ketones catalyzed by TS-1. *React. Kinet. Catal. Lett.* **2005**, *87*, 25−32.
(33) Gallo, E.; Bonino, F.; Swarbrick, J. C. Preference towards Five-Coordination in Ti Silicalite-1 upon Molecular Adsorption. *ChemPhysChem* **2013**, *14*, 79−83.
(34) Peng, H.-g.; Xu, L.; Wu, H.; Zhang, K.; Wu, P. One-pot synthesis of benzamide over a robust tandem catalyst based on center radially fibrous silica encapsulated TS-1. *Chem. Commun.* **2013**, *49*, 2709−2711.
(35) Wróblewska, A.; Fajdek, A. Epoxidation of allyl alcohol to glycidol over the microporous TS-1 catalyst. *J. Hazard. Mater.* **2010**, *179*, 258−265.
(36) Srivastava, R.; Srinivas, D.; Ratnasamy, P. CO_2 activation and synthesis of cyclic carbonates and alkyl/aryl carbamates over adenine-modified Ti-SBA-15 solid catalysts. *J. Catal.* **2005**, *233*, 1−15.
(37) Thiele, G. F.; Roland, E. Propylene epoxidation with hydrogen peroxide and titanium silicalite catalyst: Activity, deactivation and regeneration of the catalyst. *J. Mol. Catal. A: Chem.* **1997**, *117*, 351−356.
(38) Liu, X. Y.; Yin, D. L.; She, Y. Y. The Surface Acid Properties of TS-1. *Adv. Mater. Res.* **2012**, *554*−*556*, 1803−1806.
(39) Gao, X.; An, J.; Gu, J.; Li, L.; Li, Y. A green template-assisted synthesis of hierarchical TS-1 with excellent catalytic activity and recyclability for the oxidation of 2, 3, 6-trimethylphenol. *Microporous Mesoporous Mater.* **2017**, *239*, 381−389.

https://doi.org/10.1021/acsomega.2c02535
ACS Omega 2022, 7, 23851−23857